

Itinerant Ferromagnetism for Mixed Valence Systems

C. D. Batista,¹ J. Bonča,² and J. E. Gubernatis¹

¹Center for Nonlinear Studies and Theoretical Division Los Alamos National Laboratory, Los Alamos, NM 87545

²Department of Physics, FMF, University of Ljubljana and J. Stefan Institute, Ljubljana, Slovenia
(November 19, 2018)

We introduce a novel mechanism for the unusual itinerant ferromagnetism found in mixed valence systems like $\text{Ce}(\text{Rh}_{1-x}\text{Ru}_x)_3\text{B}_2$, $\text{La}_x\text{Ce}_{1-x}\text{Rh}_3\text{B}_2$, US, USe, and UTe. With it we can provide an explanation for the long-unexplained large value of T_c ($\sim 100^\circ\text{K}$) value and the maximum in the magnetization below T_c found experimentally. We also show that this novel itinerant ferromagnetism can be continuously connected with the localized case for which the energy scale is much smaller ($J_{\text{RKKY}} \sim 1^\circ\text{K}$).

Introduction. Understanding the mechanisms for ferromagnetism usually involves a reconciliation of a localized electron picture, traced back to Heisenberg [1], and an itinerant electron picture, traced back to Bloch [2]. For many insulating materials, adding itinerant features, such as indirect exchange, to the localized picture brings satisfactory agreement with basic experimental features. For many metals, adding localized features, such as spin waves, to the itinerant picture has a similar effect. On the other hand it is now appreciated that for some novel classes of materials, such as the heavy Fermion and mixed valence materials, doctoring one picture or the other is often a questionable procedure. The electrons can display both localized and itinerant properties as these materials are neither good insulators nor good metals.

In this letter we propose a simple mechanism for ferromagnetism (FM) in heavy fermion mixed valence materials. The mechanism relies on several specific energy scales set by the band structure of these materials even though the electron correlation energy is the dominant energy scale. The simplicity and generality of the mechanism however should provide a useful framework for discussing ferromagnetism in broad classes of heavy fermion mixed valence materials often found in $4f$ and $5f$ materials and their compounds. In fact we will show that it seems to explain some of the very unusual long unexplained ferromagnetic properties of such Ce based compounds as $\text{Ce}(\text{Rh}_{1-x}\text{Ru}_x)_3\text{B}_2$ [3] and the uranian monochalcogenides [4].

The mechanism is based upon a two-band structure. The lower band near the zone center is dispersive and nearly free of electron correlation effects. Away from the zone center, this band is very flat and doubly occupied states experience strong correlation effects. The upper band is separated from the lower band by a gap that is smaller than the correlation energy. When the chemical potential is at the flat band level, the system becomes unstable to the formation of a ferromagnetic state. There are compounds satisfying this mixed valence requirement under normal conditions or by either adding additional electrons (doping), applying pressure, or changing the

temperature. This ferromagnetic state is a manifestation of a Hund-like rule among electrons in band states as opposed to usual case of electrons in localized states (atomic orbitals).

We will show that the periodic Anderson model (PAM) is a simple microscopic realization of this picture. Using quantum Monte Carlo simulations, we will demonstrate that the model admits a ferromagnetic ground state in the mixed valence regime with electron occupancies reflecting our physical picture. We then develop a mean field picture that reproduces the ground state properties of the PAM and also allows us to compute finite temperature properties. Under certain conditions we find the finite temperature mean-field approximation predicts the same highly unusual behavior as a peak, below T_c , in the temperature dependence of the magnetization [3,4] and the deviation of the inverse susceptibility from Curie-Weiss behavior [5].

Model Hamiltonian. The PAM is described by the Hamiltonian

$$H = -t \sum_{\langle i,j \rangle, \sigma} (d_{i\sigma}^\dagger d_{j\sigma} + d_{j\sigma}^\dagger d_{i\sigma}) + V \sum_{i,\sigma} (d_{i\sigma}^\dagger f_{i\sigma} + f_{i\sigma}^\dagger d_{i\sigma}) + \epsilon_f \sum_{i,\sigma} n_{i\sigma}^f + \frac{U}{2} \sum_{i,\sigma} n_{i\sigma}^f n_{i\sigma}^{\bar{f}} \quad (1)$$

where $d_{i\sigma}^\dagger$ and $f_{i\sigma}^\dagger$ create an electron with spin σ in d and f orbitals at lattice site i and $n_{i\sigma}^f = f_{i\sigma}^\dagger f_{i\sigma}$ is the number operator for the f -electrons of spin σ at site i . The hopping amplitude t between d -orbitals is only to nearest-neighbor sites. The hopping amplitude V hybridizes different orbitals on the same site.

When $U = 0$, the resulting non-interacting Hamiltonian H_0 has two dispersive bands:

$$E_\sigma^\pm(\mathbf{k}) = \frac{1}{2} \left[e_{\mathbf{k}} + \epsilon_f \pm \sqrt{(e_{\mathbf{k}} - \epsilon_f)^2 + 4V^2} \right] \quad (2)$$

separated by an hybridization gap. For a chain, the band structure is illustrated in Fig. 1a. Irrespective of spatial

dimension, each band has regions where the \mathbf{k} -states are dominantly of d or f -character. A mixed valence condition arises when the Fermi energy E_F sits in a crossover region which is around the energy ϵ_f . Three energies are important: the hybridization gap Δ , the f -state dispersion $\delta_f = \partial E^- / \partial k|_{k_F} = \hbar v_F$ (v_F is the Fermi velocity), and the Coulomb (correlation) energy U . δ_f is measuring the band dispersion close to the Fermi level. In the interacting problem we will assume that $U > \delta_f, \Delta$. As we shall now discuss, the competition is between δ_f and Δ which will be a competition between a ferromagnetic and paramagnetic state.

Mechanism for Ferromagnetism. In Fig. 1a-c we illustrate the physical mechanism for the ferromagnetic state which emerges when the electron filling ρ is around 1/4 (one electron per lattice site) and the energy ϵ_f of the f -orbitals is close to E_F . The latter condition defines the intermediate valence regime.

To explain the mechanism, we first consider the non-interacting case (Fig. 1a). States in the lower band with mainly f -character have a small dispersion δ_f because of the absence of direct hopping between the f -orbitals. In the interacting case, because the Coulomb interaction only affects the electrons in the f -orbitals, the electrons which were doubly occupying the states in the lower band with mainly d -character are practically unaffected. On the other hand, the electrons in the many states which are close to the Fermi level and have mainly an f -character will be strongly affected. These electrons spread to higher unoccupied \mathbf{k} -states in the f -part of the band and polarize by an in-band Hund's rule (Fig. 1b). To see the analogy to Hund's rule more clearly, we consider the limiting case, represented in Fig. 1c, where $\delta_f = 0$ and $\Delta \neq 0$, reducing Fig. 1b to a two level system in momentum space with each level being strongly degenerate (we only plot the states with predominant f character). If we add electrons to this two levels system it is easy to show that the ferromagnetic solution has the lowest energy and is therefore the ground state. By polarizing, the spatial part of the wave function becomes antisymmetric and there is no double occupancy in the real space. In this way, the Coulomb repulsion is reduced to zero. The kinetic energy has also the lowest possible value if the electrons are occupying the lower energy (degenerated) levels (see Fig. 1c).

We now describe the conditions for the stability of the ferromagnetic state, and we will see how this mechanism departs from the one of Stoner [6]. To this end we state the condition $U \gg \Delta$. From Fig. 1b it is clear that the cost of the spreading of the ferromagnetic solution is an increase in the kinetic energy proportional to δ_f . On the other hand, if we build up a nonmagnetic solution only using the states of the lower band, there will be a minimum delocalization for each particle due to the fact that a finite set of f -character states is in the upper band (see Fig. 1). This can be seen by constructing an f Wannier function with the lower band states. This Wannier function will have a delocalization length which depends

on the \mathbf{k} wave vector where the two bands are crossing. Therefore, by localizing in real space to avoid the double occupancy, the electrons will have a finite probability of occupying the f -states in the upper band. The energy cost per electron of occupancy is proportional to Δ . If the hybridization gap is much larger than the dispersion of the states, that is, $\Delta \gg \delta_f$, the ferromagnetic state lies lower in energy than the nonmagnetic state. The energy of the excited nonmagnetic state is proportional to Δ . This can be easily seen from the limiting (and non-realistic) case $\delta_f = 0$ plotted in Fig. 1c, for which the analogy with the atomic shells and the Hund's rule is evident.

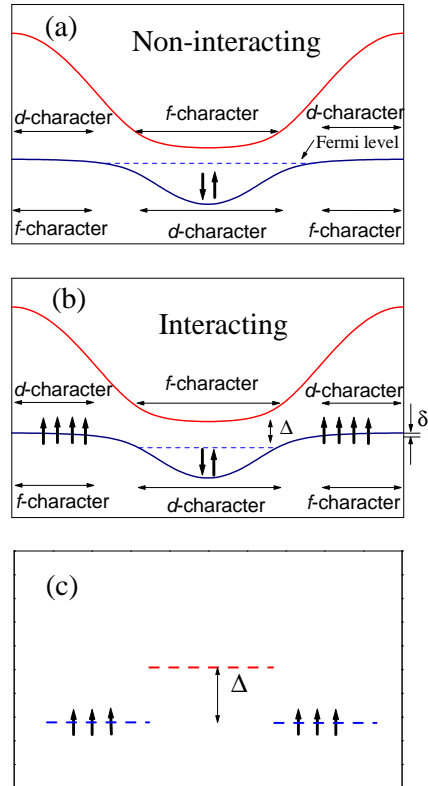


FIG. 1. Illustration of the ferromagnetic mechanism.

It is important to emphasize that the hybridization gap Δ and f -state dispersion δ_f are the two basic ingredients of our mechanism: Δ only appears if there is more than one band and δ_f is small only if the hybridization is weak. If $U > \Delta, \delta_f$, then Δ is the energy scale of the paramagnetic state, while δ_f is the energy scale of the ferromagnetic solution. We can estimate the magnitude of these scales for the PAM: for $V \lesssim t/2$, we get $\delta_f \sim \partial e_k / \partial k|_{k_F} V^2 / (e_{k_F} - \epsilon_f)^2$ and $\Delta \sim V^2 / (2dt - \epsilon_f) + \sqrt{(2dt + \epsilon_f)^2 + 4V^2} - 2dt$. Therefore, if ϵ_f is close to the bottom of the lower band ($\epsilon_f + 2dt \sim t$) and the Fermi level is close to the top ($E_F \sim \epsilon_f - V^2 / (2dt - \epsilon_f)$), Δ is considerably larger than δ_f and the ground state is ferromagnetic. We can see that the ferromagnetic solution is stable for comfortably realistic values of the parameters. It is clear from this

analysis the particle density ρ for a ferromagnetic solution must be close to quarter filling.

Quantum Monte Carlo Method. Using the constrained-path Monte Carlo method (CPMC), we computed the ground-state properties of the PAM on a square lattice. The CPMC method projects the ground state from an initial state $|\psi_T\rangle$ by converting the iterative procedure

$$|\psi_{i+1}\rangle = e^{-\tau H}|\psi_i\rangle \quad (3)$$

into a branched random walk. The details of the method are described elsewhere [7] as are our prior uses of it on the square PAM [8,9].

The defining characteristic of the CPMC method is its elimination of the fermion sign problem by excluding random walkers $|\phi\rangle$ that violate $\langle\psi_T|\phi\rangle > 0$. If $|\psi_T\rangle$ were the exact ground state $|\psi_0\rangle$, this constraint would generate an exact elimination of the sign problem, and hence an exact solution. Extensive benchmarking indicates the CPMC method provides accurate estimates of the energy and various correlation functions.

We prepared the trial state in specific values of the total spin and z-component of spin [9]. Because the Hamiltonian(1) conserves these quantum numbers, the iterative process (3) produces a ground state with the same S and S_z . In the ferromagnetic regime, when the number of lattice sites N was greater than the number of electrons N_e , the resulting energy as a function of S almost always showed a minimum at a value of S satisfying $0 < S < \frac{1}{2}(2N - N_e)$. Hence we typically found a partially polarized ferromagnetic ground state.

For square lattices we also computed dependence of the static spin structure factor and the electron occupancies both on position and wave number space [8]. Most notable for the present work is the wave vector dependence of the different spin components of the upper and lower band electron occupancies shown in Fig. 2. It has the same quantitative features as Fig. 1b.

Mean Field Theory. The quantum Monte Carlo simulations are limited to chains and square lattices of relatively small sizes at zero temperature. However, we have found that their predictions are well described by a simple spin-polarized mean-field approximation. We can easily extend this approximation to larger systems sizes in higher dimensions and at finite temperatures. We can use large lattices in three-dimensions at finite temperatures to compare with the results of experiments.

The mean field Hamiltonian H_{MF} is

$$H_{MF} = H_0 + \frac{U}{2} \sum_{i,\sigma} (\langle n_{i\sigma}^f \rangle n_{i\bar{\sigma}}^f + n_{i\sigma}^f \langle n_{i\bar{\sigma}}^f \rangle - \langle n_{i\sigma}^f \rangle \langle n_{i\bar{\sigma}}^f \rangle) \quad (4)$$

$\langle n_{i\uparrow}^f \rangle$ and $\langle n_{i\downarrow}^f \rangle$ are determined in a self-consistent way within the mean-field theory. The translational symmetry of H implies that we can always find a translationally invariant ground state. This means that $\langle n_{i\uparrow}^f \rangle$ and $\langle n_{i\downarrow}^f \rangle$

will not depend on the site index i . Therefore there are two variational parameters to be determined from the mean-field equations: $\langle n_{\uparrow}^f \rangle$ and $\langle n_{\downarrow}^f \rangle$.

Even though the mean field approximation can give a good description of the FM ground state, it is well known that such approximations overestimate the energy of the paramagnetic phase because they improperly estimate the real space correlations that are very important for the paramagnetic solution. Therefore it is crucial to check that the ground state is the FM one by using a more accurate method to evaluate the energy of the PM state. To this end we calculated the ground state of the PAM with 6×6 unit cells using the CPMC technique. We found excellent agreement with the energy and as seen in Fig. 2 the electron occupancies.

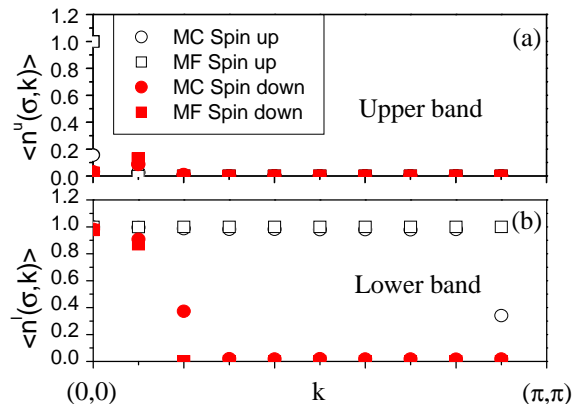


FIG. 2. Comparison between Mean Field and CPMC values of the occupation numbers of the non-interacting band states for each spin polarization in a 6×6 cluster ($\rho = 7/24, V = 0.5t, U = t$, and $\epsilon_f = -3t$). On the x -axis we only include the nonequivalent wave vectors ordered according to increasing non-interacting energies.

Consequences. Bolstered by this agreement we used the mean-field approximation to calculate various thermodynamic properties of the ferromagnetic phase for the three-dimensional cubic PAM. In Fig. 3a we show the temperature dependence of the magnetization for different values of ϵ_f . From the arguments given above it is clear that the magnetization comes from the electrons which are occupying the states with f -character. By increasing ϵ_f we are reducing the number of f -electrons and therefore the magnitude of the zero temperature magnetization. Some critical value of ϵ_f exists where the chemical potential starts departing from ϵ_f and a new energy scale $\epsilon_f - E_F$ emerges in the system. This new energy scale is reflected in the appearance of a magnetization peak. (See the $\epsilon_f = -t$ case in Fig. 3a.) To understand the last statement one first has to realize that the zero temperature magnetization is small due to the reduction of the number of f -electrons. When the temperature is of the order of $\epsilon_f - E_F$, electrons are promoted from the double occupied band states to the f -character states which have a large entropy (large density of states). The f -electrons will be polarized due to the energy con-

siderations above explained. In this way we can explain the origin of the magnetization peak below T_c . It is important to note that the source for the large entropy is associated with charge and not with spin degrees of freedom. This fact explains why a state with larger magnetization has a higher entropy. The magnetization curves shown in Fig. 3a are in good qualitative agreement with the magnetization versus temperature data measured in $\text{Ce}(\text{Rh}_{1-x}\text{Ru}_x)_3\text{B}_2$ for different values of x [3].

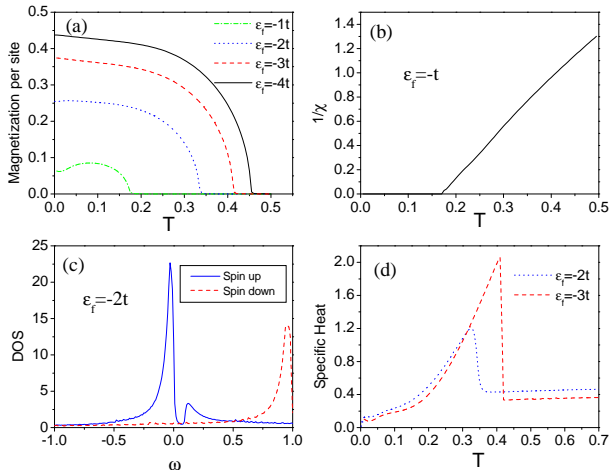


FIG. 3. Mean field results ($\rho = 1/4, V = 0.5t, U = 2t$) for (a) magnetization, (b) inverse susceptibility, (c) density of states and (d) specific heat.

Another interesting aspect of this ferromagnetism is the deviation from linearity (Curie-Weiss behavior) for the inverse magnetic susceptibility above T_c over a large temperature range (see Fig. 3b) [5]. The behavior contrasts that predicted by theories based on localized magnetic moments.

From above it is also clear that the change in entropy from the magnetic to the paramagnetic phase depends on the number for f electrons (spin degrees of freedom). This dependence is seen in Fig. 3d where we plot the calculated specific heat for different values of ϵ_f .

A characteristic of this ferromagnetic state that has consequences for the photoemission experiments is the implication that the quasi-particle dispersion should be close to that of the electrons in the non-interacting case. We recall that the ferromagnetic state described in Fig. 1 is very similar to a non-interacting polarized state. As in the Stoner mechanism, the main role of the Coulomb repulsion is to polarize states with well defined momentum. The hybridization gap of the noninteracting solution is most likely replaced by a pseudogap (see Fig. 3c). This pseudogap should be seen in the optical conductivity measurements.

Conclusions. Our quantum Monte Carlo simulations and mean-field calculations clearly show the existence of an itinerant ferromagnetic phase in mixed valence materials that is supported by the PAM. This new phase describes qualitatively many experimental features such as an unusually large value for T_c ($\sim 100^\circ\text{K}$) and the max-

imum in the magnetization below T_c [10] that are found in such ferromagnetic compounds as $\text{Ce}(\text{Rh}_{1-x}\text{Ru}_x)_3\text{B}_2$ [3], $\text{Ce}(\text{Rh}_{1-x}\text{Os}_x)_3\text{B}_2$ [3], and $\text{La}_x\text{Ce}_{1-x}\text{Rh}_3\text{B}_2$ [10].

Many previous theories of $4f$ and $5f$ electron materials treated these materials as systems of localized moments in the f -orbitals. These theories are thus unable to describe an itinerant ferromagnetic phase and experimental consequences [4] like the peak in the magnetization below T_c observed in some of these systems [3,5], the large value of T_c , the deviation of $\chi^{-1}(T)$ from the Curie-Weiss law above T_c in the uranium monochalcogenides [5], and the mixed valence behavior of these compounds [10,13,14].

The physical picture just presented, when combined with our previous results [9], allows a reconciliation of the localized and delocalized ferromagnetism pictures painted by Heisenberg and Bloch seventy years ago in the sense that it is possible to go continuously from the mixed valence FM state where the f -electrons are delocalized to a FM state where there is one localized electron in each f -orbital [9]. In our picture one can do this by decreasing ϵ_f from the Fermi level to a value near or below the bottom of the valence band. We note that the energy scale of a localized ferromagnetic state is that of the RKKY interaction, which according to de Gennes's rule [11] is of the order of 1°K , while the scale for the itinerant case introduced here is that of the hybridization gap Δ , which is of the order of 100°K for heavy fermion compounds [12]. In going from the delocalized (mixed valence) to the localized regime we thus expect a strong reduction of T_c accompanied by an increase of the zero temperature magnetization. (The $T = 0$ magnetization is proportional to the f occupation number.) This expectation is consistent with the observed behavior of the magnetization in $\text{La}_x\text{Ce}_{1-x}\text{Rh}_3\text{B}_2$ as function of x [10].

Acknowledgements. This work was sponsored by the US DOE under contract W-7405-ENG-36. We acknowledge useful discussions with A. J. Arko, B. Brandow, M. F. Hundley, J. J. Joyce, J. M. Lawrence, S. Trugman, and J. L. Smith. In particular, we thank J. M. Lawrence for pointing out the experimental work on the Ce compounds. J. B. acknowledges the support Slovene Ministry of Education, Science and Sport, Los Alamos National Laboratory and FERLIN.

-
- [1] W. Heisenberg, Z. Physik **49**, 619 (198).
 - [2] F. Bloch, Z. Physik **57**, 545 (1929).
 - [3] S. K. Malik, A. M. Umarji, G. k. Shenoy, and M. E. Reeves, Phys. Rev. B **31**, 4728 (1985).
 - [4] P. Santini, R. Lémanski, and P. Erdos, Advan. in Phys. **48**, 537 (1999).
 - [5] V. I. Chechernikov, A. V. Pechennikov, E. I. Yarembash, L. F. Martinova, and V. K. Slavyanskikh, Sov. Phys. JETP **26**, 328 (1968).

- [6] E. C. Stoner, *Phil. Mag.* **15**, 1018 (1933).
- [7] Shiwei Zhang, J. Carlson and J. E. Gubernatis, *Phys. Rev. Lett.*, **74**, 3652 (1995); *Phys. Rev. B* **55**, 7464 (1997); J. Carlson, J. E. Gubernatis, G. Ortiz, and Shiwei Zhang, *Phys. Rev. B* **59**, 12788 (1999).
- [8] J. Bonča and J. E. Gubernatis, *Phys. Rev. B* **58**, 6992 (1998).
- [9] C. Batista, J. Bonča, and J. E. Gubernatis, *Phys. Rev. B*, to appear (cond-mat/0009128).
- [10] S. A. Shaheen, J. S. Schilling, and R. N. Shelton, *Phys. Rev. B* **31**, 656 (1985).
- [11] P.-G. de Gennes, *Comm. Energie At. (France) Rappt.* **925**, (1959).
- [12] This change in the energy scale of both ferromagnetic states is obtained with Monte Carlo by taking the energy difference between the PM and the FM solutions at $T = 0$. The mean field theory is not appropriate to describe this transition because it overestimates the PM energy.
- [13] M. A. Kanter and C. W. Kazmierowicz, *J. Appl. Phys.* **35**, 1053 (1954).
- [14] M. Erbudak and J. Keller, *Z. Phys. B* **23**, 281 (1979).